3D Kirchhoff migration using wavelet transform

Valery A. Zheludev

School of Mathematical Sciences Tel Aviv University, Ramat Aviv 69978, Israel and Company Paradigm Geophysical Ltd. Herzlia, 46120, Israel

Eugene Y. Ragoza

Company Paradigm Geophysical Ltd. Herzlia, 46120, Israel

Dan D. Kosloff

Dept. of Earth and Planetary Sciences Tel Aviv University, Ramat Aviv 69978, Israel and Company Paradigm Geophysical Ltd. Herzlia, 46120, Israel

Valentin I. Meshbey

Company Paradigm Geophysical Ltd. Herzlia, 46120, Israel

(January 6, 2004)

ABSTRACT

We developed fast wavelet based algorithm for 3D Kirchhoff imaging leaning upon the time-frequency localization property of mathematical wavelets. Our approach consists in the migration of the wavelet expansion coefficients rather than single samples as in conventional Kirchhoff migration implementation. Practically, the wavelet transform of each trace from a seismic volume is conducted, then the significant wavelet coefficients are migrated according to their time location in a manner sim-

ilar to the conventional migration of samples. These operations should be followed by a proper reconstruction. Our reconstruction algorithm handles stretching which wavelets acquire in the process of migration and includes antialiasing procedures. Since the number of migrated wavelet coefficients is much fewer than the number of samples in the time domain, the computation time can be significantly reduced. A series of 2D and 3D experiments with synthetic and real data was conducted to check whether the migration of the wavelet coefficients leads to the correct result. Results from synthetic data as well as field data have shown that the migration in the wavelet domain significantly reduces computation time while maintaining good image quality.

INTRODUCTION

Kirchhoff prestack migration of reflection data is a very important subsurface imaging tool, especially in situations where CMP stacking fails. The main advantages of Kirchhoff migration are speed and flexibility, as it can readily handle irregular survey geometry. In spite of these advantages, 3D prestack migration can be a very time consuming process. Consequently there is a big incentive to improve its performance.

This work is an attempt to improve the speed of Kirchhoff migration by utilizing the wavelet transform. The first utilization of wavelets in the seismic industry was for data compression. This allowed for a big saving in data storage, (Donoho et al., 1995), (Vassiliou and Wickerhauser, 1997). However in applications the data had to be uncompressed before being used in processing, (Bradley et al., 1996). In our opinion, a more promising approach is to implement seismic imaging directly on the wavelet coefficients. There have been a number of attempts to use wavelets in seismic imaging:(Wu et al., 1997), (Wang and Wu, 1998), (Li et al., 1998). In (Wu et al., 1997) the approach of the authors consists of the representation of the Kirchhoff migration operator matrix in the wavelet rather than in the space domain. By this means, the matrix gains sparseness, which promises, in principle, some reduction of the migration

time. However, in that work the simplifying assumption of a homogeneous background is employed and the extension to a realistic velocity variation appears very difficult, if possible at all. Li et al., (1998), suggested an approach which is somewhat related to the approach we propose. They used as atoms the standard mathematical wavelets of a fixed shape, and conducted the migration of these atoms as spikes. In their implementation the library of available waveforms was depleted which led to reduction in quality. This was because the events of interest on a trace can vary widely in shape and frequency content. The simplification of the procedure did not lead to a significant improvement in speed. One reason was that very large computational expense was required to extract the atoms to be migrated. Furthermore, the locations of the atoms on traces were unpredictable, thus complicating the calculation of the travel-time tables. The reconstruction of atoms after migration suggested by the authors also lead to distortion of the target image, especially in the upper layers. A different approach to migration of compressed data appears in the work of Bouska and Gray, (1998). The authors propose retaining the samples for migration from the original data traces that represent local extreme. After migration they reconstruct output traces by convolving the migrated samples with a single wavelet. The algorithm is applied to depth migration. However, the authors admit that they were not successful with run time savings. Moreover, the migrated image which they obtained, was inferior to the image from conventional migration.

We developed a fast and flexible wavelet based algorithm for 3D seismic Kirchhoff imaging leaning upon the time-frequency localization property of mathematical wavelets. Our approach consists in migration of the wavelet expansion coefficients rather than single samples as in conventional Kirchhoff migration implementation. It is equivalent to the migration of the corresponding wavelets as units. Unlike Li et al., (1998), we use the set of wavelets corresponding to different decomposition scales. Practically, the temporal wavelet transform of each trace of a seismic volume is conducted, then the significant wavelet coefficients are migrated according to their

time location in a manner similar to the conventional migration of samples. These operations would fail unless they were followed by a proper reconstruction. Our reconstruction algorithm handles stretching which wavelets acquire in the process of migration and also includes antialiasing procedures. Since the number of migrated wavelet coefficients is much fewer than the number of samples in the time domain, the computation time can be significantly reduced. We conducted a series of 2D and 3D experiments with synthetic and real data to check whether the migration of significant wavelet coefficients leads to a correct result. Results from synthetic data as well as field data have shown that the migration in the wavelet domain significantly reduces computation time while maintaining good image quality.

In the following sections we first briefly describe elements of the wavelet expansion theory, which are relevant to the Kirchhoff migration of this study. We then present the details of the migration algorithm itself. Finally the migration algorithm is tested against synthetic and real data examples. The results are compared to corresponding results from conventional Kirchhoff migration.

PRELIMINARIES

Wavelet transform

By now the wavelet transform and its extension, the wavelet packet transform, have gained wide spread use and their basics are described comprehensively in literature (Daubechies, 1992), (Mallat, 1999), (Wickerhauser, 1994). This section reviews elements of the orthogonal wavelet transform, which are relevant to the wavelet migration of this study.

Consider a discrete input signal f of length $n = 2^j$. The application of the first level of the wavelet transform on it results in two groups of expansion coefficients, each of size $n/2$ which respectively correspond to a high pass H and a low pass L

filter application on the data.

Each filter operation consists of the convolution of the signal f with the filter coefficients, followed by downsampling by a factor of two. The filters H and L form a pair of conjugate mirror filters (Mallat, 1999) which means that the convolution of the low pass filter coefficients (or the high pass coefficients) with themselves is zero for non-zero even sample values. The convolution of the high with the low pass filter coefficients is zero for all even sample values. Consequently the set of copies of the low pass filters with even sample shifts from one to the other, together with the set of high pass filters with even sample shifts, forms an orthogonal expansion basis of dimension n.

The basic advantage of the wavelet transform is the multiscale representation of a signal. The procedure described above gives the first decomposition scale. To extend the decomposition to subsequent scales, the transform is carried out recursively. Namely, the high pass H and the low pass L filters are applied to the low pass expansion coefficients of the previous scale, followed by downsampling. After m iterations the signal is decomposed into blocks of coefficients:

$$f \longrightarrow Hf \bigcup HLf \bigcup HLLf \ldots \bigcup HL^{m-1}f \bigcup L^m f.$$

The number of coefficients in the k^{th} block is $n/2^k$, while in the m^{th} block there are $n/2^m$ high pass coefficients and in the last $(m+1)^{th}$ block there are $n/2^{m+1}$ low pass coefficients.

The inverse wavelet transform is started from the blocks $HL^{m-1}f$ and $L^m f$ belonging to the lowest decomposition scale. They are upsampled by the factor of two, convolved with the filters H^T and L^T respectively and summed with each other. As a result, the low frequency block of the upper scale $L^{m-1}f$ is produced. Then the procedure is repeated using the blocks $HL^{m-2}f$ and $L^{m-1}f$ producing the low frequency block $L^{m-2}f$. Before the final step of reconstruction the low-frequency Lf and the high-frequency Hf blocks are available. Applying the above procedure to

these blocks, we recover the signal f.

An alternative perspective of the process described is the decomposition of the original signal into a wavelet basis. When only one of the expansion coefficients is non- zero, the result of application of the inverse transform is the wavelet centered at the appropriate time, and stretched to the scale of the level of the non-zero coefficient. Therefore, each expansion coefficient is the weight of a wavelet in the signal at a given time and scale. By this means the wavelet transform presents both temporal and spectral information. The magnitude of an expansion coefficient corresponds to the presence of the wavelet at the appropriate scale in the original signal at a certain time. Conversely, the coefficient also indicates the presence of the frequency bandwidth of the stretched wavelet at that time.

In Figure 1 we display the blocks of the transform coefficients corresponding to the decomposition of a seismic signal into 5 scales. In Figure 2 we display the result of partial reconstruction of the signal from each decomposition scale. In Figure 3 the Fourier transforms of these partial reconstructions are depicted. By this means we illustrate the contributions of blocks of coefficients into the signal in either the time or the frequency domain.

In Figures 4- 5 we depict wavelets corresponding to 5 decomposition scales and their Fourier spectra. The wavelets were generated using the filters related to the splines of fourth order. It is seen that the wavelets are well localized in both the time and the frequency domains. Passage from an upper scale to the lower one results in approximately two times dilation of the wavelet and two times shrinkage of its frequency band. Therefore the frequency bands of the wavelets split the frequency domain along with the logarithmic scale.

Remarks:

1. By now the highly efficient algorithms of the wavelet transform and new types of wavelets are available (Sweldends , 1996), (Averbuch et al., 2000), (Averbuch,

Pevnyi, Zheludev, 2000).

2. In Figures 1- 3 a property common to seismic signals is manifested. It can be seen that some scales prevail over the others. This means that essential information on the structure of signals is contained mostly within these scales.

3. Location of significant wavelet coefficients corresponds to location of events of interest within signals. A small coefficient placed at some point indicates that the fragment of the signal located in the vicinity of the point does not correlate with the corresponding wavelet. As it is seen from Figure 1, the majority of coefficients are of small magnitude. Their removal could reveal the essential structure of the signal rather than corrupt it.

Kirchhoff migration.

The wavelet transform enables the representation of seismic data in compressed form where only coefficients of significant magnitude are maintained. This fact is used to construct a Kirchhoff prestack time migration algorithm, which operates directly on the expansion coefficients of the one dimensional temporal wavelet transform of the seismic traces. For typical unstacked reflection seismic data, the one-dimensional wavelet transform allows a relatively modest data compression ratio of about 3- 4. However, with a proper design, a comparable speedup of the migration algorithm can be achieved.

Kirchhoff time migration consists of summing sample values from the input traces (with a multiplication by an appropriate weight factor) into the output traces. Given a shot located at $(x_s, y_s, z_s = 0)$ on the surface, a receiver located at $(x_r, y_r, z_r = 0)$ and an output trace at (x, y) (Figure 6), the relation between input time t_{in} and migrated time t_{mig} is given by the double square root equation:

$$t_{in} = \sqrt{t_{mig}^2 - 4\left(\frac{(x-x_s)^2 + (y-y_s)^2}{\nu^2}\right)} + \sqrt{t_{mig}^2 - 4\left(\frac{(x-x_r)^2 + (y-y_r)^2}{\nu^2}\right)} \quad (1)$$

where $\nu(x, y, t_{mig})$ is the rms velocity. The input sample $p_{in}(x_s, y_s, x_r, y_r, t_{in})$ is cumulated into the output migrated sample $p_{mig}(x, y, t_{mig})$. The scheme is illustrated in Figure 6.

WAVELET MIGRATION

General approach

The migration scheme of this study maps the wavelet expansion coefficients according to Equation (1) in an identical manner to which the input time samples in ordinary Kirchhoff migration are mapped.

As mentioned, unlike the Fourier transform, the wavelet expansion possesses the temporal information where each expansion coefficient corresponds to a given time value. The migration maps the input expansion coefficients into the expansion coefficients of the output.

In the implementation we used the orthogonal wavelet basis generated by the splines of fourth order (Mallat, 1999). The decomposition is carried out to four levels. One of characteristic features of our algorithm is that, unlike the conventional wavelet transform, we use only the low frequency coefficients from the blocks Lf, LLf, $LLLf$, $LLLLf$. These blocks correspond to 1/2, 1/4, 1/8 and 1/16 of Nyquist cutoff frequency respectively. We depict in Figure 7 these blocks of coefficients for the real seismic signal which was displayed above. Figure 8 displays the reconstruction from these blocks, and in Figure 9 we show the Fourier spectra of the reconstructed blocks. Corresponding wavelets and their spectra are displayed in Figure 10 and in Figure 11.

The wavelet migration differs from conventional Kirchoff migration in the manner in which migration stretch and spatial aliasing are handled. Migration stretch is caused by the fact that when an input trace is mapped into an output trace, two

consecutive samples of the output originate from two input values which are separated by a smaller increment in time than a time sample. Mathematically,

$$stretch \;=\; \frac{dt_{mig}}{dt_{in}} \quad .$$

For example for zero offset migration $stretch \;=\; t_{in}/t_{mig}$. The stretch factor depends on the time and on the location of the input trace with respect to the output trace. As a rule, the stretching decreases with an increase in time, and increases with an increase in the angle between the output location and the shot-receiver midpoint. Migration stretch is a common feature of all migration algorithms and normally does not require special treatment except perhaps for muting. However, stretching requires special consideration in the wavelet migration. In our implementation, a discrete set of stretch factors are predefined. For a given output time and spatial location, the corresponding input sample value is mapped into the output at the nearest stretch factor level. The migration results for each stretch value are calculated separately. Only after the reconstruction of the output from the wavelet coefficients the results from all stretch levels are combined by stacking.

For a shot-receiver pair, the image at an output location is cumulated only from the input coefficients from one scale. The selection of the particular scale is done according to a spatial aliasing criterion. In this manner the migration emulates the antialiasing procedure in standard Kirchhoff migration, where a number of copies of the input trace, each with a different degree of high cut filtering, are used.

Due to the handling of stretching and spatial aliasing, different outputs are created at each location. The total number of outputs equals the number of stretch factors used times the number of wavelet decomposition levels. Although each wavelet decomposition level has its inherent sampling rate, all the migration mapping is carried out to the original sampling rate of the input trace. The reconstruction of the migration output from the migrated wavelet coefficients is done by a correlation with the

filter coefficients at that sampling rate.

The main gain in computation speed compared to the conventional Kirchhoff migration comes from the reduction of the number of the input samples. Most of the upper portion of the seismic section is migrated in the coarsest expansion scales with large sampling rates and, correspondingly, with a small number of samples. In the deeper levels, as well, the use of the coefficients from the first decomposition scale (block Lf) reduces the number of samples by two. In application on real data, in most cases, the wavelet migration has been faster than ordinary Kirchoff migration by a factor of four to five.

EXAMPLES

2D synthetic example

A synthetic 2D seismic section (Figure 12) was used for the first series of experiments. It consisted of 300 traces each containing 1024 samples. It was an example of a zero-offset section with a CMP spacing of 20m and the time sampling $\Delta t = 4\ msec.$ The propagation velocity was assumed constant and equal to 2000 m/sec. The section was generated from a model containing five flat reflectors with dips varying between 20^o and 60^o respectively.

The migrated section is shown in Figure 13. The migration was carried out with a depth step of 4m. using only the block LLf of the wavelet coefficients (the low-pass expansion coefficients of the second scale). No antialiasing treatment was applied. As the figure shows, the migration was able to image all the reflectors correctly.

Example of prestack migration of a 3D real data volume

We demonstrate results of prestack time migration of a 3D real data survey. The survey contained 281 inlines, each of which had 361 traces. Each trace had 748

samples with a sampling rate of 4 msec. The maximal source-receiver distances were 2525 m. along the inline direction and 3024 m. along the crossline direction. The average fold was 15.

Figure 14 displays a section along one inline produced by conventional Kirchhoff time migration. Figure 15 shows results from the same line using the wavelet migration described in previous section. One can observe that the obtained image is very close in quality to the image from the conventional migration. However, in this example, the wavelet migration took half the CPU time as the ordinary migration.

CONCLUSION

We presented an adaptation of Kirchhoff prestack time migration to operate on wavelet expansion coefficients of the one-dimensional wavelet transform of the input data. After the wavelet expansion, the migration is carried out in an identical manner to ordinary Kirchhoff migration. As the number of expansion coefficients of significant value is always smaller than the number of input time samples, less samples need to be moved from the input to the output, thus enabling an improvement in computational speed.

The wavelet migration has been tested against a 2D synthetic example as well as against 3D field data examples. The results were quite satisfactory and comparable in quality to those of ordinary Kirchhoff time migration. However, use of the wavelet expansion required some compromises like for example the grouping of the stretch factor into discrete categories, or the relatively simple antialiasing scheme. Therefore we anticipate situations where this migration will be used for preliminary evaluations and velocity determination, while conventional Kirchhoff migration will be used for obtaining the final best image.

In the paper we presented the first stage of our investigation. The objective was to carry out the migration in the wavelet domain and to achieve the improvement in

computational speed staying as much as possible within techniques of conventional migration. Therefore, while the achieved acceleration is comparatively moderate, the developed scheme could be immediately incorporated into existing migration software.

In future investigations we intend to examine more flexible tools based on the wavelet packet transform. Moreover we intend to link the migration procedures with modern data compression and coding techniques (Averbuch et al., 2000), (Said and Pearlman, 1996).

ACKNOWLEDGEMENTS

The research supported by the grant of Israel Science Foundation –1999-2003, No.258/99-1, *Application of the Wavelet Transform to 3D Seismic Imaging.*

REFERENCES

Averbuch, A. Z., Meyer, F. G., Stromberg, J.-O., 2000, Fast adaptive wavelet packet image compression,IEEE Trans. on Image Processing, **9**, 792-800.

Averbuch, A. Z., Pevnyi A. B., Zheludev V. A., Butterworth wavelets derived from discrete interpolatory splines, Preprint,www.math.tau.ac.il/∼amir (∼zhel).

Borac, S. and Seiler, R., 1997, Loop group factorization of biorthogonal wavelet bases, Preprint.

Bouska, J. G. and Gray, S., 1998, Migration of unequally sampled compressed seismic data, 68th Ann. Internat. Mtg., Soc. Expl. Geophys., Expanded Abstracts, 1128-1130.

Bradley, J. Fei, T. and Hildebrand, S., 1996, Wavelet compression for 3D migration, 66th Ann. Internat. Mtg., Soc. Expl. Geophys., Expanded Abstracts, 1627-1629.

Daubechies, I., 1992,Ten lectures on wavelets. SIAM.

Donoho, P. L., Ergas, R. A., and Villasenor, J. D., 1995, High-performance seismic trace compression, In Proceedings of SEG, 160-163.

Li, Xin-Gong, Wang, B., Pann, K., Anderson, J. and Deng, L., 1998, Fast migration using a matching pursuit algorithm, 68th Ann. Internat. Mtg., Soc. Expl. Geophys., Expanded Abstracts, 1732-1735.

Mallat, S., A wavelet tour on signal processing, Academic Press.

Said, A. and Pearlman, W. A., A new fast and efficient image codec based on set partitioning in hierarchical trees. IEEE Trans. on Circ. and Syst. for Video Tech., **6(3)**, 243-250.

Sweldends, W. , The lifting scheme: A custom design construction of biorthogonal wavelets, Appl. Comput. Harm. Anal. **3(2)**, 186–200.

Vassiliou, A. and Wickerhauser, M. V., 1997, Comparison of wavelet image coding schemes for seismic data compression, 67th Ann. Internat. Mtg., Soc. Expl. Geophys., Expanded Abstracts, 1334-1337.

Wang, Y. and Wu, Ru-Shan, 1998, Migration operator decomposition and compression using a new wavelet packet transform:beamlet operator, 68th Ann. Internat. Mtg., Soc. Expl. Geophys., Expanded Abstracts, 1167-1170.

Wickerhauser, M. V., 1994, Adapted Wavelet Analysis from Theory to Software, AK Peters, Wellesley, Massachusetts.

Wu, Ru-Shan, Yang, F., Wang, Z. and Zhang, L., 1997, Migration operator compression by wavelet transform: beamlet operator, 67th Ann. Internat. Mtg., Soc. Expl. Geophys., Expanded Abstracts, 1646-1649.

FIGURES

FIG. 11. Fourier transforms of the wavelets displayed in Figure 10.

FIG. 12. A synthetic 2D seismic section.

FIG. 13. Wavelet migration of the synthetic 2D seismic section shown in Figure 12.

FIG. 14. Conventional prestack migration of a 3D real data survey.

FIG. 15. Wavelet prestack migration of the 3D real data survey.

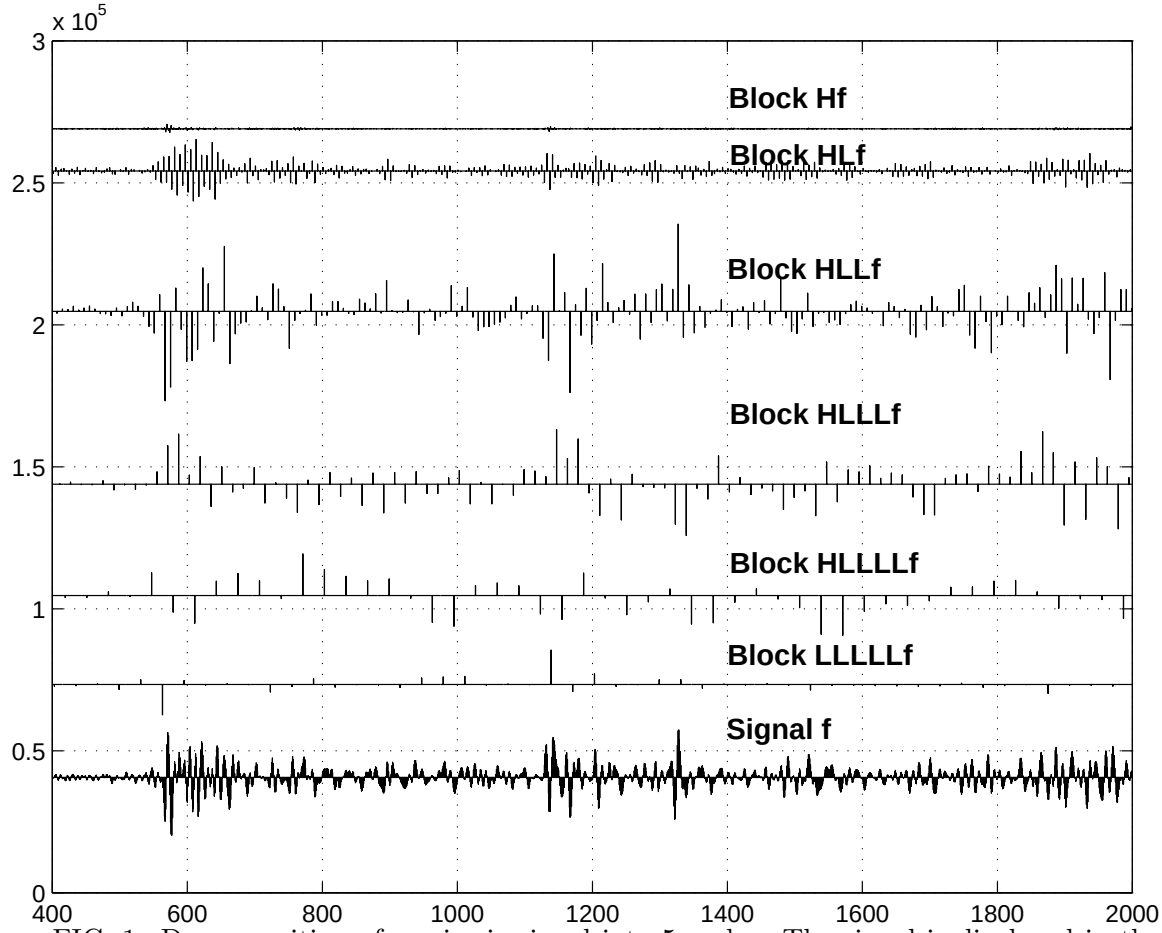

FIG. 1. Decomposition of a seismic signal into 5 scales. The signal is displayed in the bottom plot.

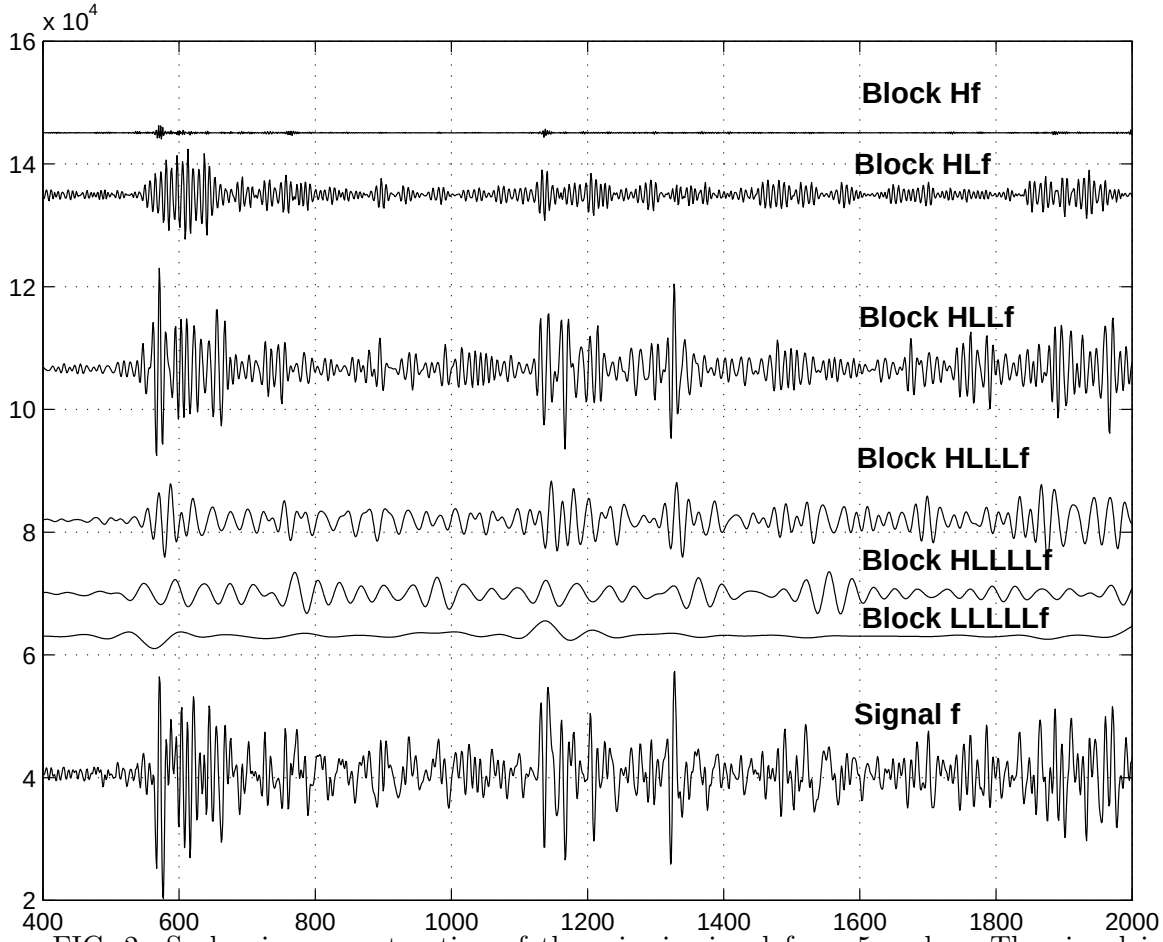

FIG. 2. Scale-wise reconstruction of the seismic signal from 5 scales. The signal is displayed in the bottom plot.

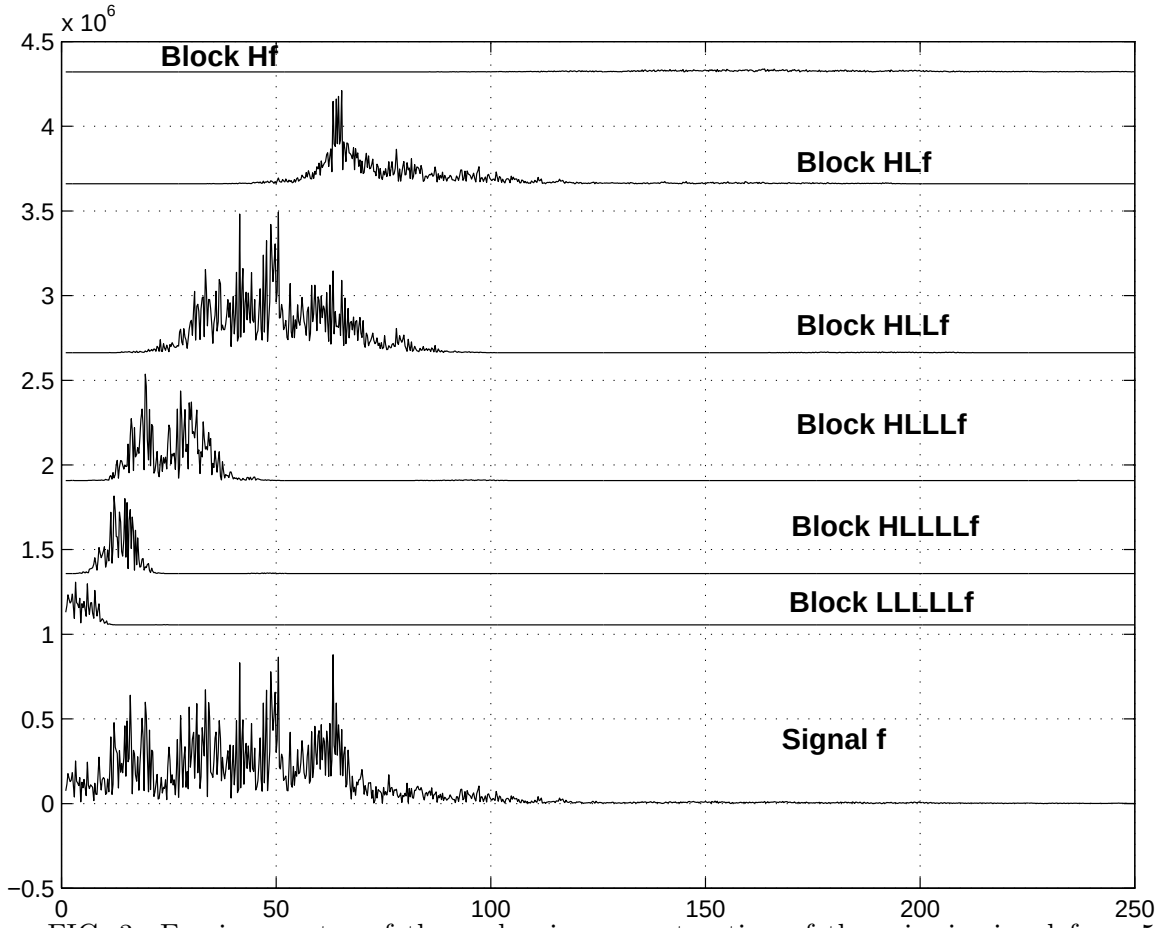

FIG. 3. Fourier spectra of the scale-wise reconstruction of the seismic signal from 5 scales. The spectrum of the signal is displayed in the bottom plot.

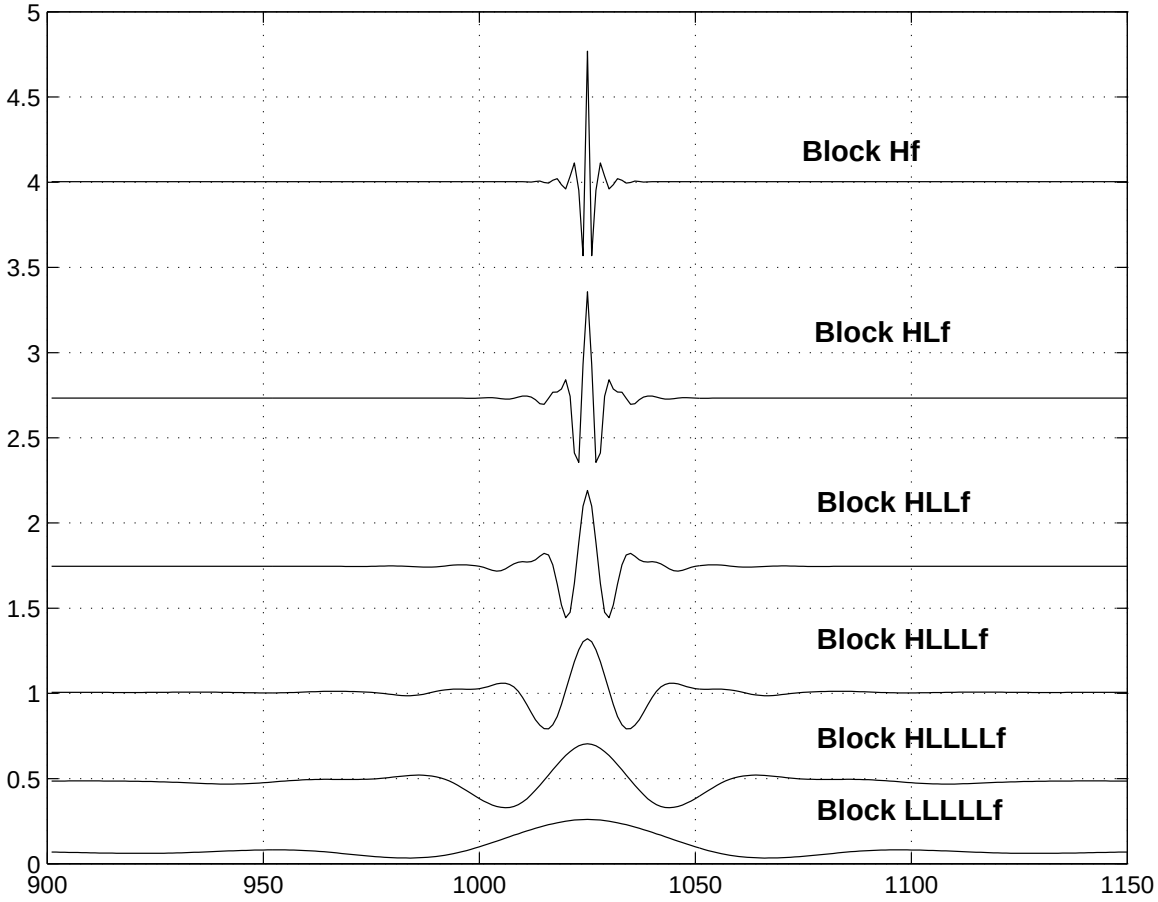

FIG. 4. Wavelets corresponding to 5 decomposition scales.

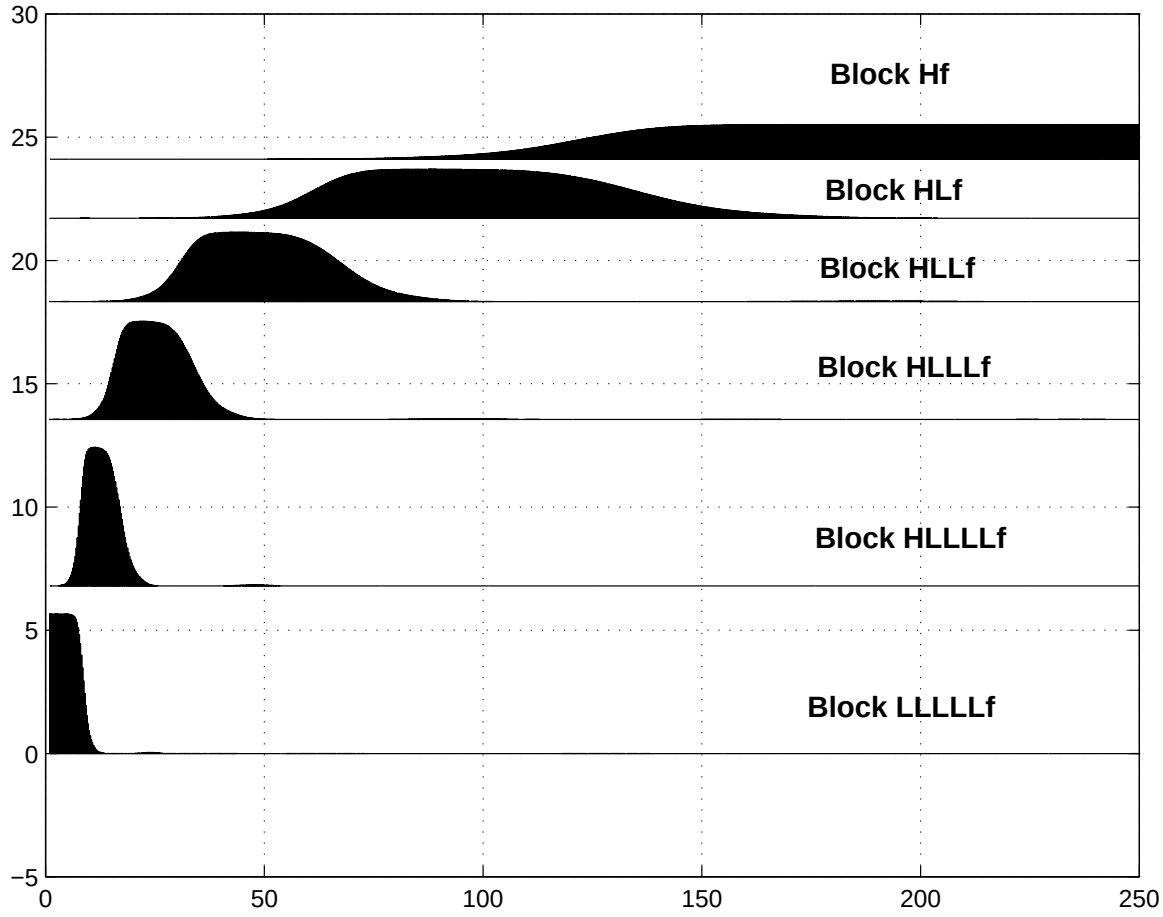

FIG. 5. Fourier spectra of the wavelets depicted in Figure 4.

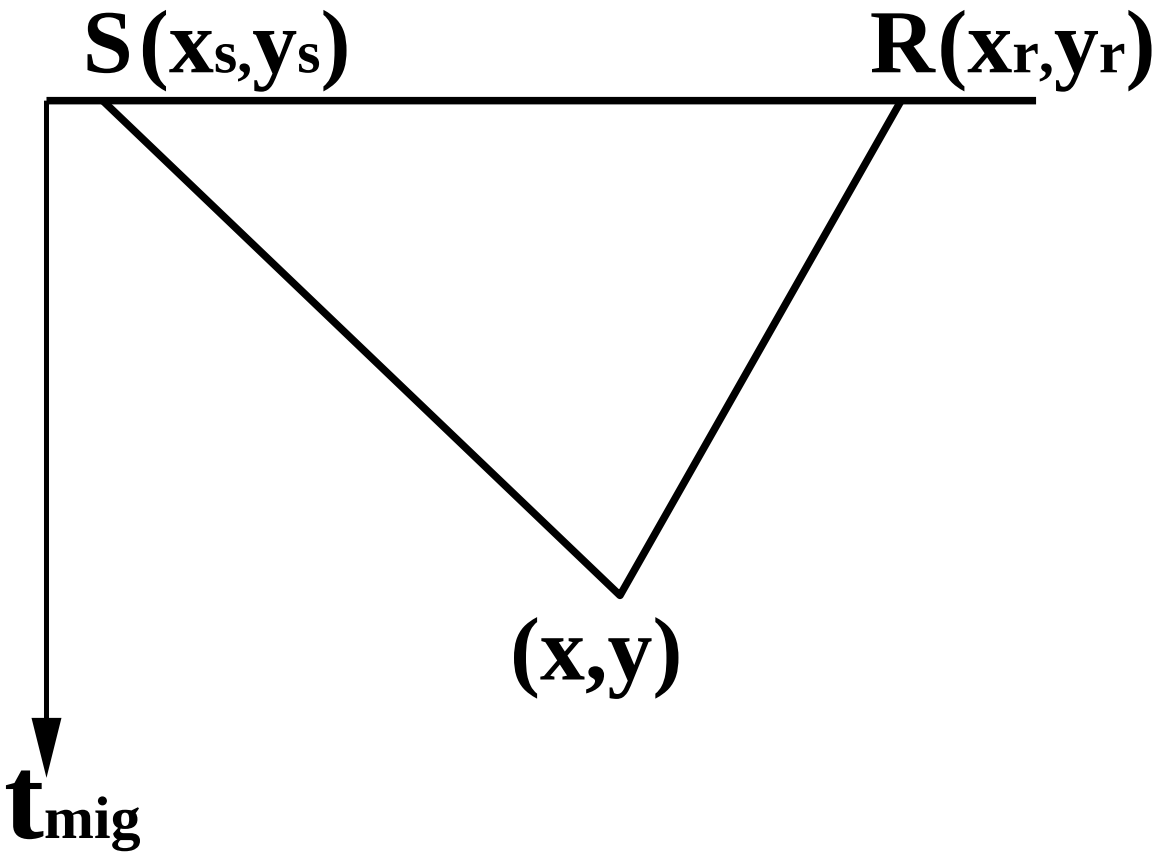

FIG. 6. Scheme of Kirchhoff migration.

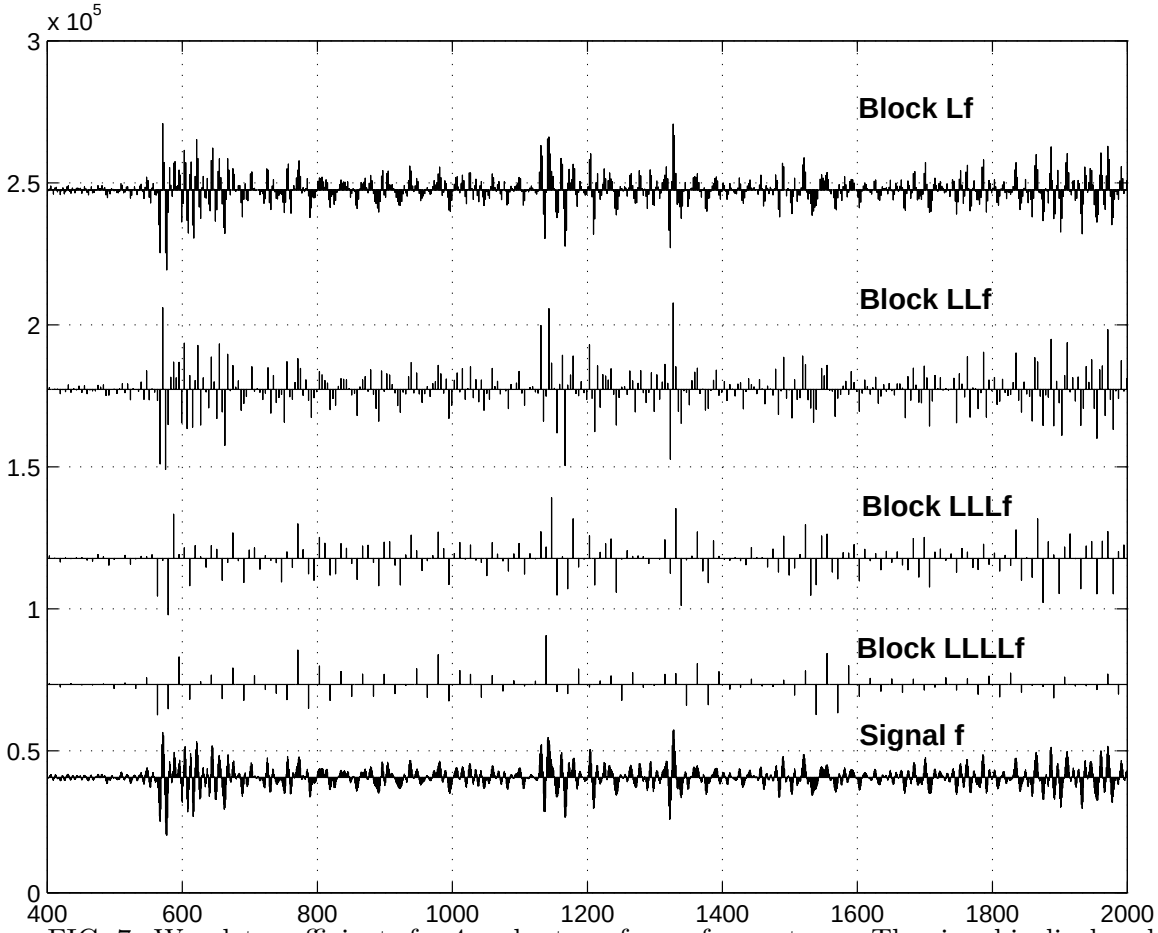

FIG. 7. Wavelet coefficients for 4 scales transform of a sea trace. The signal is displayed in the bottom plot.

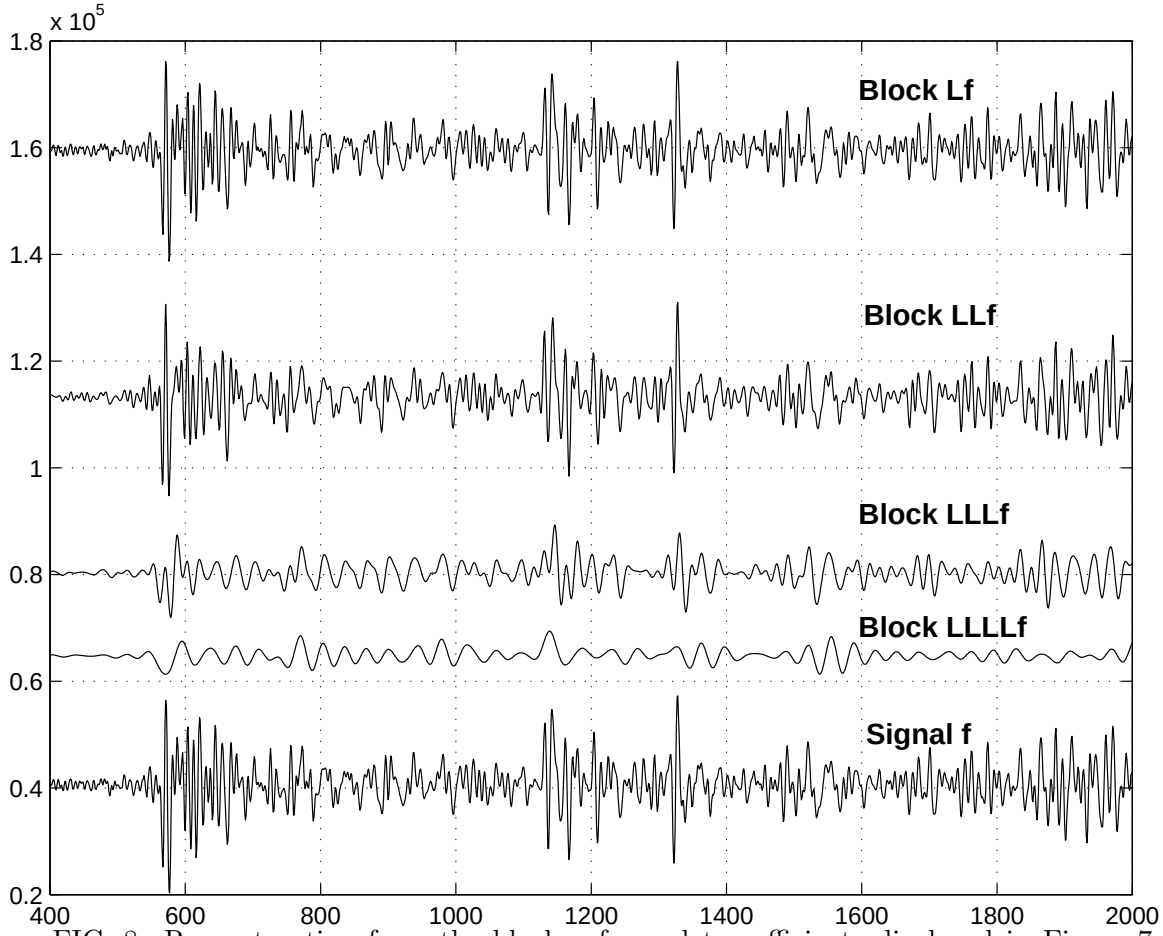

FIG. 8. Reconstruction from the blocks of wavelet coefficients displayed in Figure 7. The signal is displayed in the bottom plot.

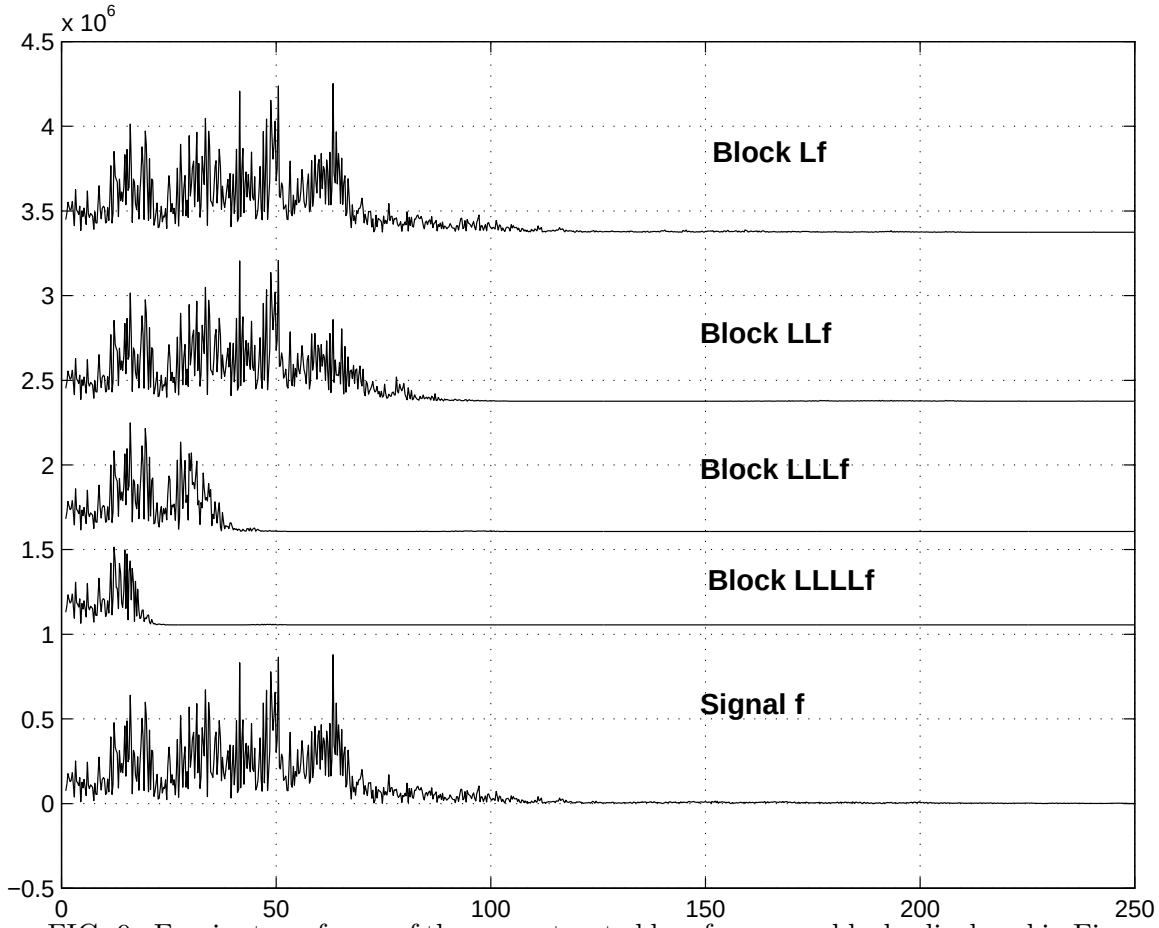

FIG. 9. Fourier transforms of the reconstructed low-frequency blocks displayed in Figure 8. The spectrum of the signal is displayed in the bottom plot.

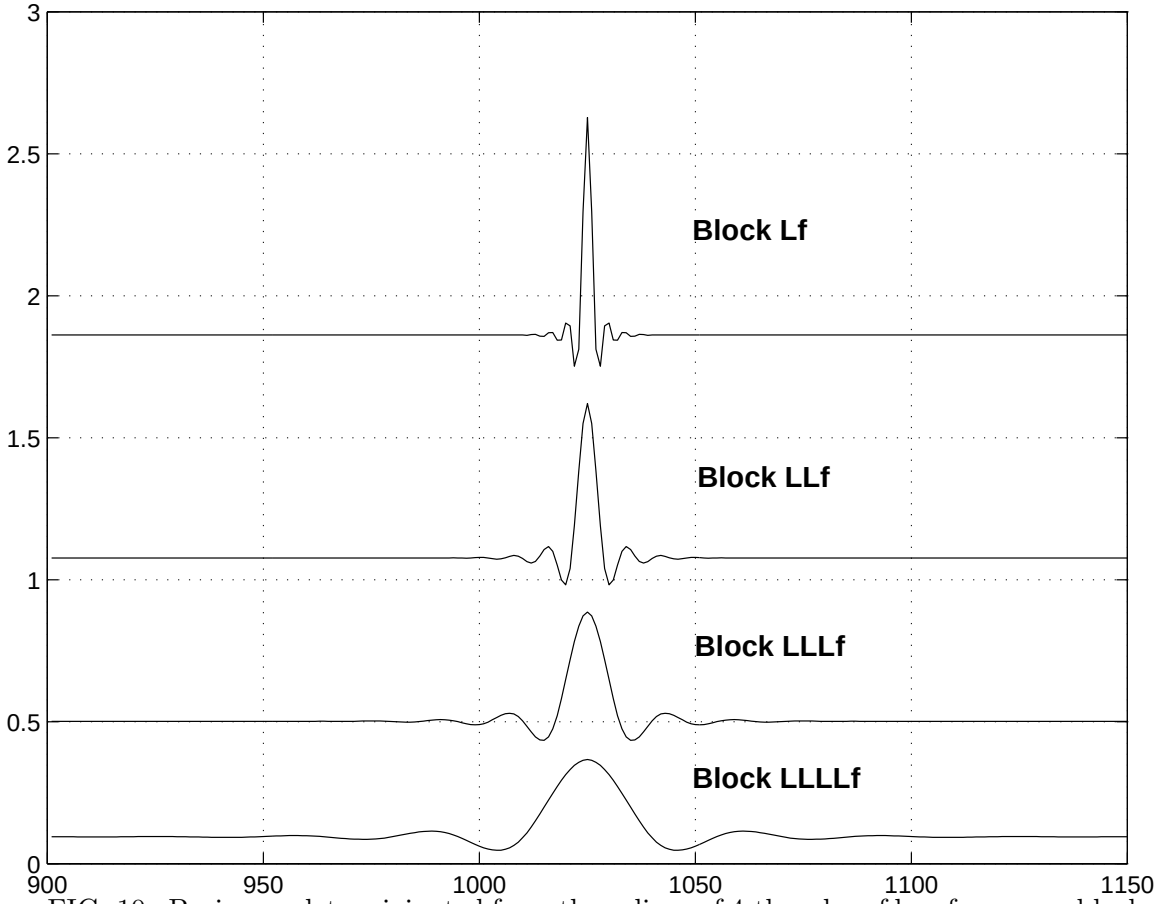

FIG. 10. Basic wavelets originated from the splines of 4-th order of low-frequency blocks for 4 scales of wavelet transform .

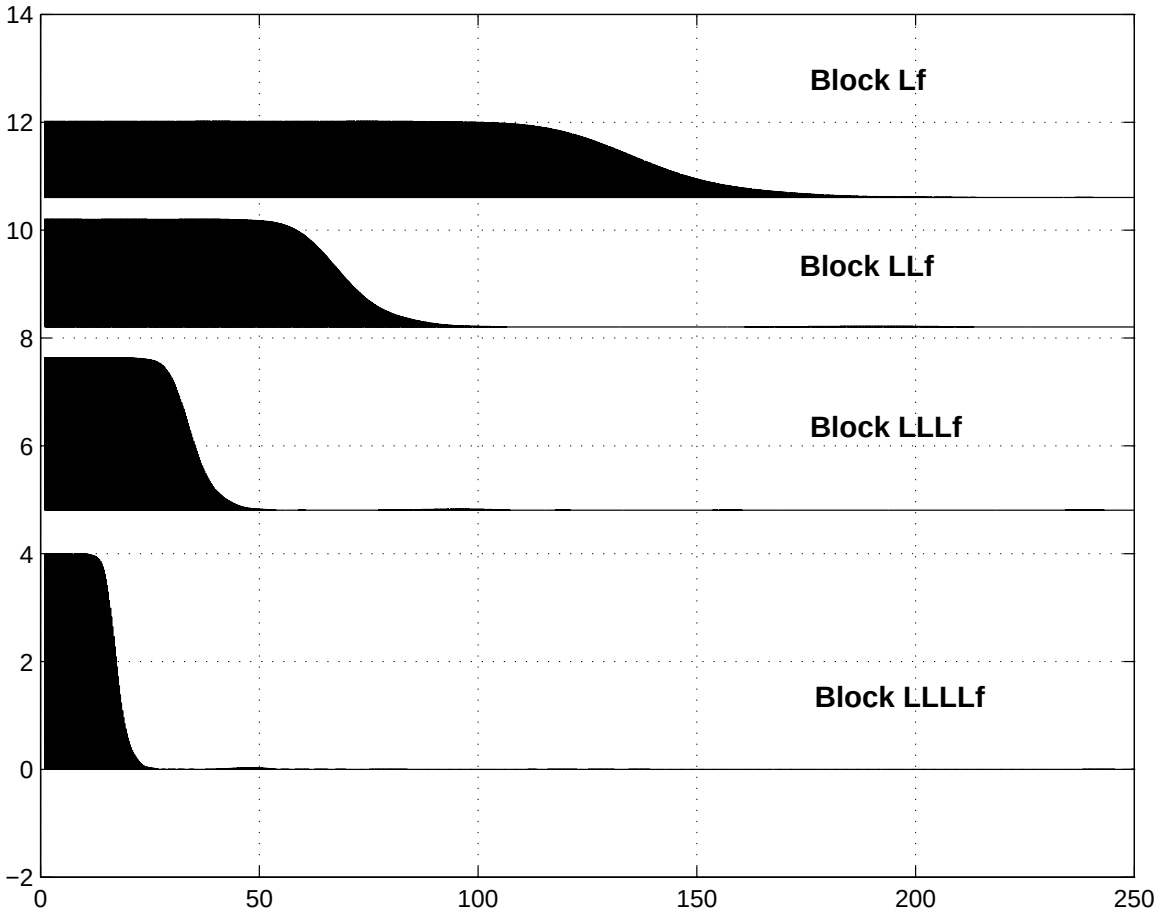

FIG. 11. Fourier transforms of the wavelets displayed in Figure 10.

FIG. 12. A synthetic 2D seismic section.

FIG. 13. Wavelet migration of the synthetic 2D seismic section shown in Figure 12.

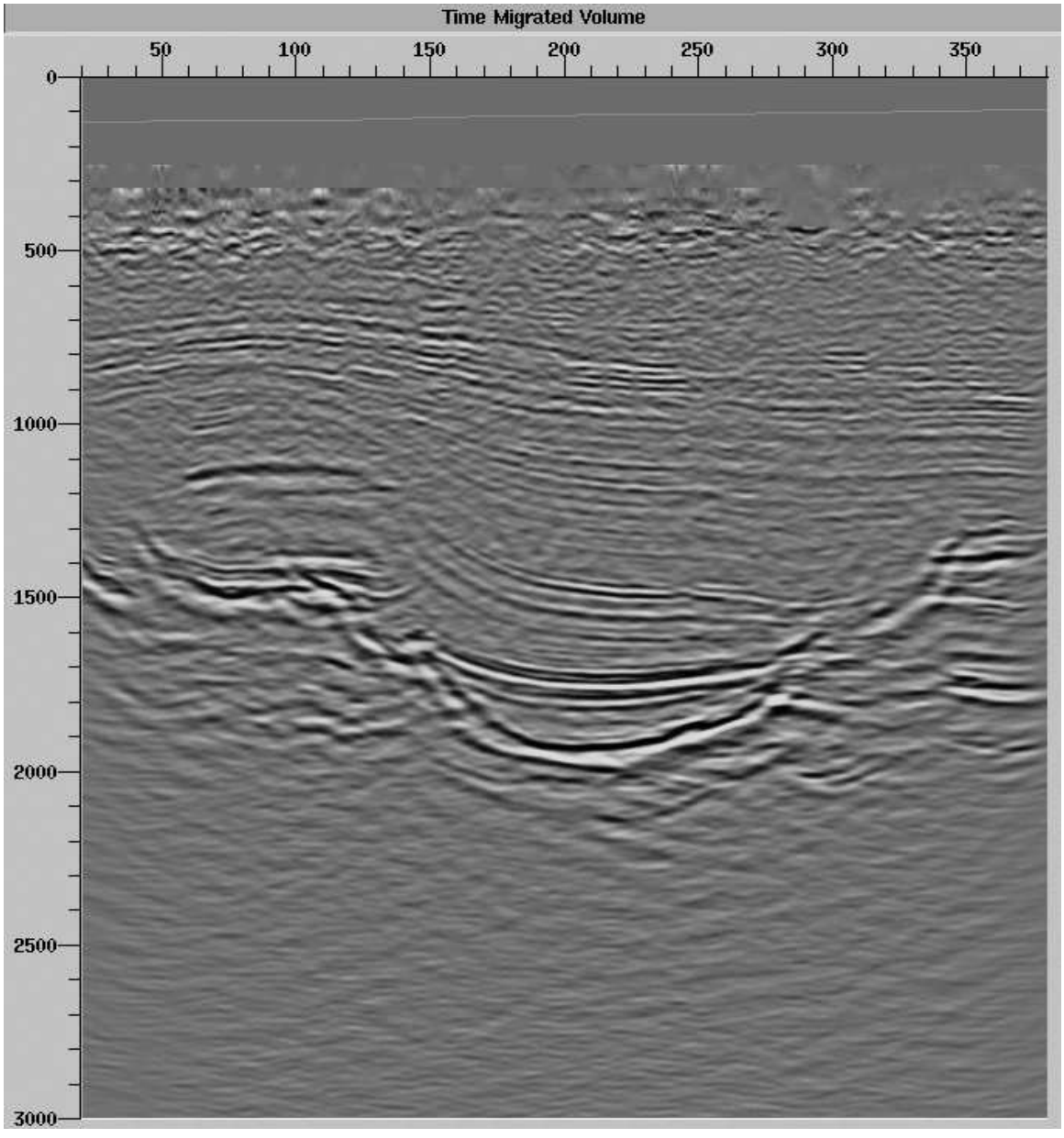

FIG. 14. Conventional prestack migration of a 3D real data survey.

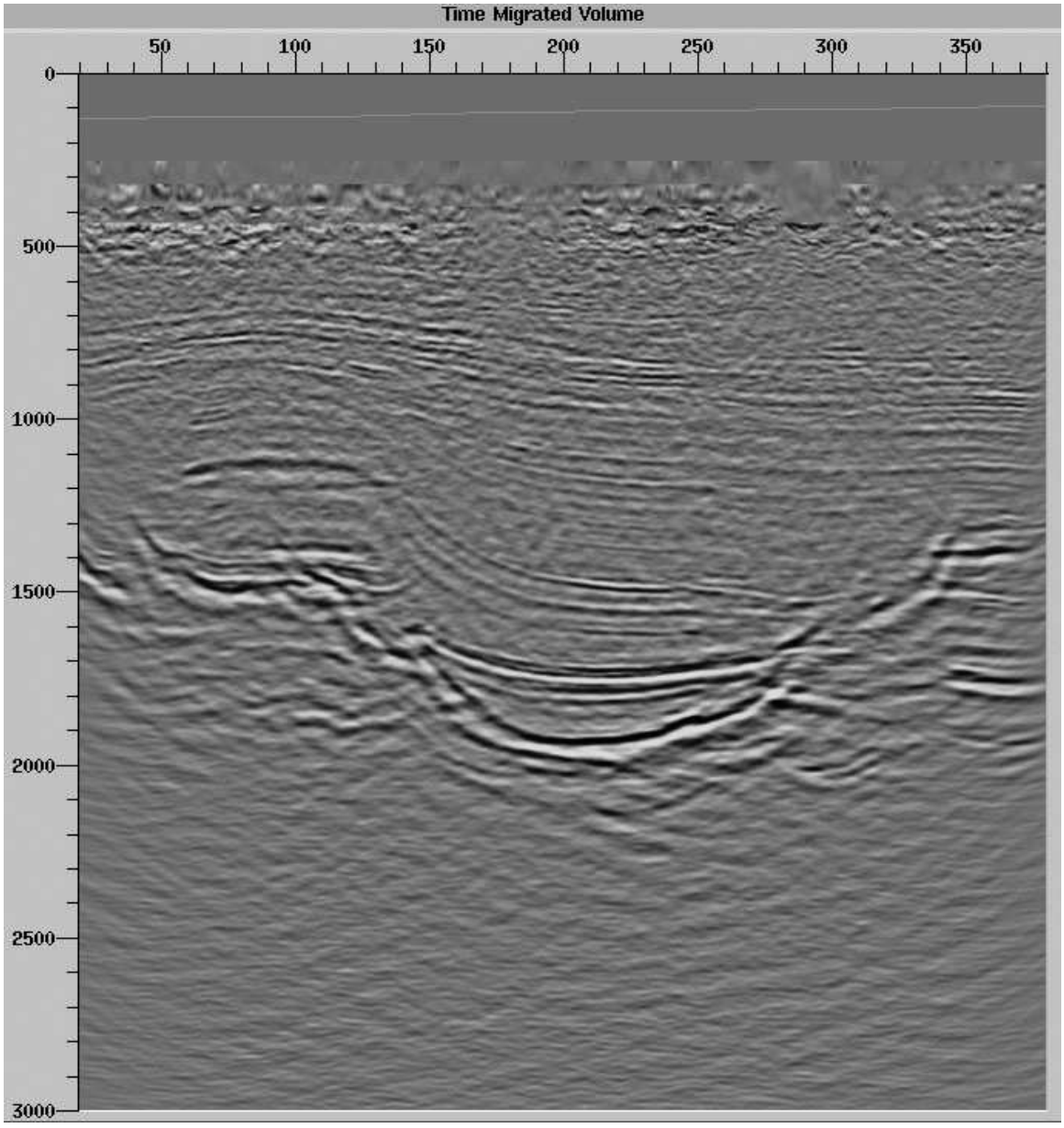

FIG. 15. Wavelet prestack migration of the 3D real data survey.